

File ID uvapub:144512  
Filename 6: Low-molecular-weight model study of peroxide cross-linking of EPDM rubber using gas chromatography-mass spectrometry : addition and combination  
Version final

---

SOURCE (OR PART OF THE FOLLOWING SOURCE):

Type PhD thesis  
Title Characterisation of polymeric network structures  
Author(s) R. Peters  
Faculty FNWI: Van 't Hoff Institute for Molecular Sciences (HIMS), FNWI: Swammerdam Institute for Life Sciences (SILS)  
Year 2009

FULL BIBLIOGRAPHIC DETAILS:

<http://hdl.handle.net/11245/1.293831>

---

*Copyright*

*It is not permitted to download or to forward/distribute the text or part of it without the consent of the author(s) and/or copyright holder(s), other than for strictly personal, individual use, unless the work is under an open content licence (like Creative Commons).*

---

## 6

## Low-molecular-weight model study of peroxide cross-linking of EPDM rubber using gas chromatography and mass spectrometry.

## Addition and combination

**Abstract**

The dicumyl-peroxide-initiated addition and combination reactions of mixtures of alkanes (*n*-octane, *n*-decane) and alkenes (5,6-dihydrodicyclopentadiene (DCPDH), 5-ethylidene-2-norbornane (ENBH) and 5-vinylidene-2-norbornane (VNBH)) were studied to mimic the peroxide cross-linking reactions of terpolymerised ethylene, propylene and a diene monomer (EPDM). The reaction products of the mixtures were separated by both gas chromatography (GC) and comprehensive two-dimensional gas chromatography (GC×GC). The separated compounds were identified from their mass spectra and their GC and GC×GC elution pattern. Quantification of the various alkyl/alkyl, alkyl/allyl and allyl/allyl combination products show that allylic-radicals comprise approximately 60% of the substrate radicals formed. The total concentrations of the products formed by combination are found to be independent of the concentration and the type of alkene. In addition, the total concentration of the formed addition products depends strongly on the type of the alkene used, *viz.* VNBH > ENBH ≈ DCPDH, which is a consequence of differences in steric hindrance of the unsaturation. The peroxide curing efficiency, defined as the number of moles of cross-linked products formed per mol of peroxide, is 173% using 9% (*w/w*) VNBH. This indicates that the addition reaction is recurrent. In addition, the present results provide more-detailed structural information. The described approach to use low-molecular-weight model compounds has proven to be a very powerful tool to study the cross-linking of EPDM.

*R. Peters, M. van Duin, D. Tonoli, G. Kwakkenbos, Y. Mengerink, R. van Benthem, C.G. de Koster, P. Schoenmakers, Sj. van der Wal, Journal of Chromatography A, 1201 (2008) 151-160.*

## 6.1. Introduction

EPDM rubber is an elastomer, which is terpolymerised from ethylene, propylene and a diene monomer. Due to its excellent resistance to heat, ozone, oxygen and water, it can be used for a wide range of outdoor and demanding applications [1]. It dominates the market for non-tyre rubber applications (*e.g.* window or door sealing). EPM (a copolymer of ethylene and propylene) can be cross-linked with peroxides, but the introduction of a diene ter-monomer strongly improves the cross-linking efficiency. The two dienes commonly used in commercial EPDM are dicyclopentadiene (DCPD) and 5-ethylidene-2-norbornene (ENB) (*Fig. 6.1*) [2]. Recently a new advanced catalyst technology was developed, which enables the incorporation of up to 3% (*w/w*) of 5-vinylidene-2-norbornene (VNB) (*Fig. 6.1*) into EPDM, without the occurrence of polymer-reactor fouling or excessive polymer branching [3]. The concentration and the type of the diene significantly influence the peroxide curing efficiency. It has been shown that the curing efficiency is governed by steric effects [4]. VNB is the most efficient diene for peroxide curing [5], while ENB and DCPD have similar but lower reactivities. Although the type and the concentration of the incorporated diene are important parameters, the ethylene/propylene ratio, the molecular weight distribution of the EPDM, the degree of EPDM branching, the use of co-agents/additives, and the cure temperature also influence the peroxide cross-linking efficiency [4].

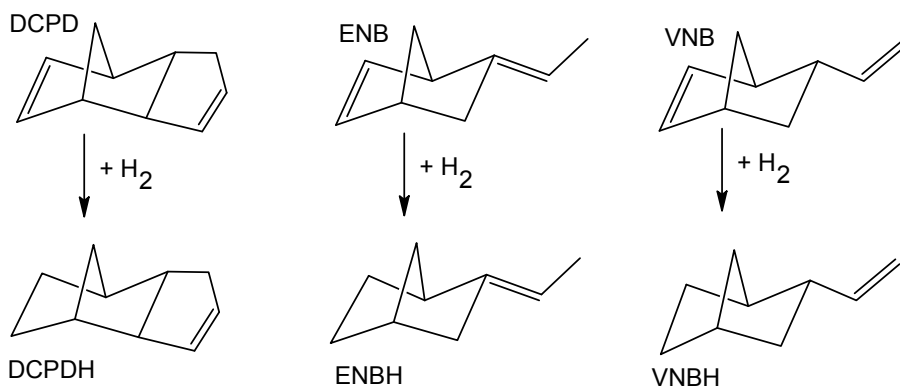


*Fig. 6.1. The chemical structure of the different EPDM dienes and their corresponding hydrogenated model compounds.*

Knowledge of the chemical nature of the cross-links and of the cross-link

density is important for understanding the physical properties of peroxide cross-linked EPDM. Solid-state nuclear-magnetic resonance spectroscopy, infrared spectroscopy, and equilibrium swelling are important techniques to determine the diene conversion and the cross-link density [6,7,8,9]. The use of these techniques has led to a generally accepted scheme for peroxide cross-linking [4] that is shown in *Fig. 6.2*. The formation of cross-links results from the combination of macro-radicals, generated by the thermal decomposition of the peroxide, and from the addition of macro-radicals to the unsaturated moieties in EPDM.

Identification of the chemical nature and quantification of the concentration of the cross-links formed will increase the understanding of peroxide cross-linking. The poor analytical accessibility of highly cross-linked EPDM (not soluble in any solvent; no chromophores) in combination with the relatively low concentration of cross-linking structures, makes the analysis of the chemical structure of the formed networks by spectroscopic and/or chromatographic techniques rather difficult. Useful information on the chemical structure of the formed cross-links can be obtained by studying low-molecular-weight model compounds to mimic the cross-linking of the high molecular weight polymers, as shown in several studies [4,10,11]. In our previous study [12] we demonstrated the feasibility of this approach by using low-molecular-weight (methyl-) alkanes to study the combination reaction of peroxide cross-linked EP(D)M. Linear and branched alkanes were “cross-linked” to “high” molecular weight alkanes. The isomeric reaction products have been analysed by both gas chromatography–mass spectrometry (GC–MS) and comprehensive two-dimensional GC–MS (GC×GC–MS) analyses. The identification of these products based on their MS-fragmentation patterns was quite complex, due to the high tendency of random rearrangements. This resulted in very similar MS-spectra for the different branched isomeric alkanes. To increase the reliability of the MS-identification, comprehensive two-dimensional GC–MS (GC×GC–MS) was used. This technique is based on two consecutive GC separations, typically according to boiling point and polarity. It allows group-type separations according to chemical classes, which results in ordered chromatograms [13,14,15]. Although GC×GC is not necessary to improve the separation, the use of GC×GC resulted in different groups of peaks that are characteristic for the various alkane reaction products. The combination of this highly structured GC×GC chromatogram and MS-detection has resulted in proposed structures for the different isomeric reaction products. The identified reaction products gave valuable insight into the combination reactions of the alkanes. The quantification of the different branched products allowed calculation of the

selectivity for hydrogen abstraction from the different types of C-H bonds. The results were consistent with an electron spin resonance spectroscopy study on similarly “cross-linked” low-molecular-weight model compounds [11].

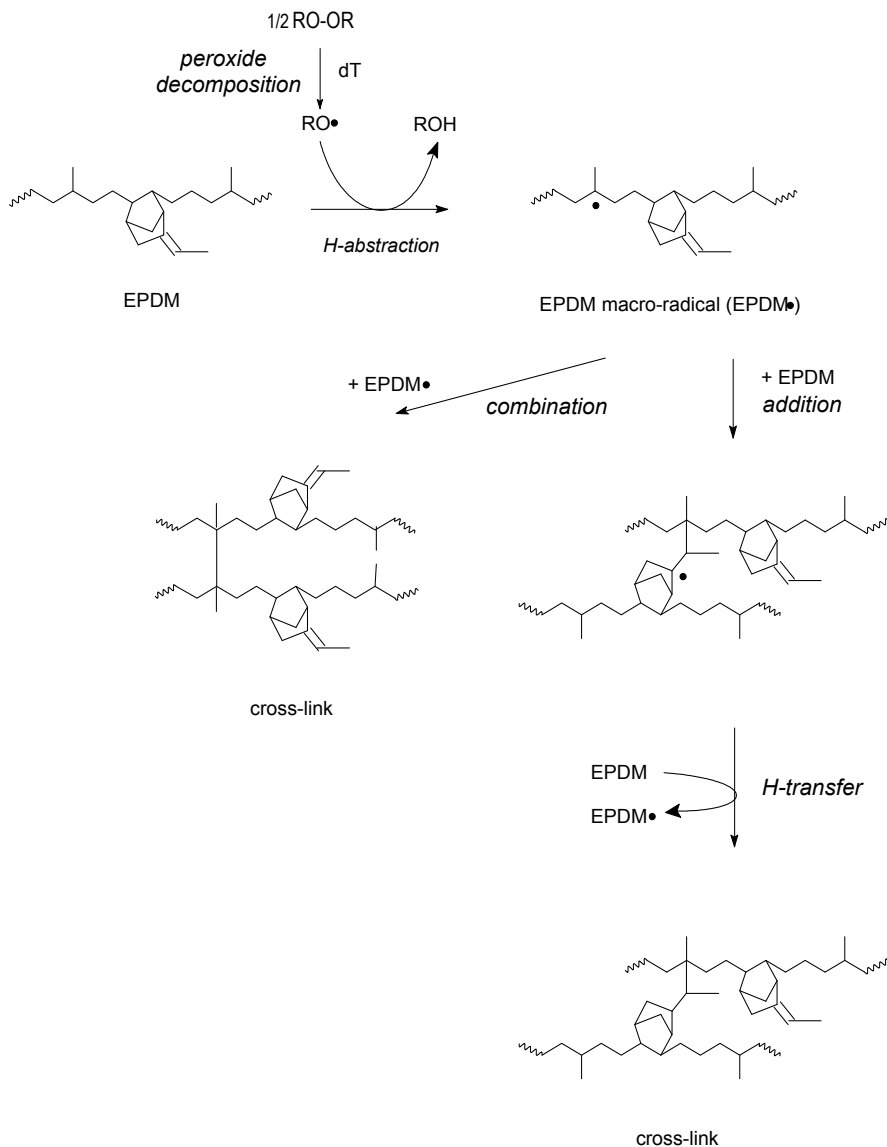


Fig. 6.2. General scheme for peroxide cross-linking of EPDM with ENB as a diene.

In this second part of our study into the peroxide cross-linking mechanism of EPDM, addition reactions are studied. The goal is to use the products and

reaction pathways identified for the addition reactions of alkenes as a model for the addition reactions that occur during peroxide curing of EPDM. Dicumylperoxide (DCP) was used to “cross-link” mixtures of low-molecular-weight alkanes and alkenes, under reaction conditions as close as possible to those used for the actual peroxide cross-linking of EPDM. As low-molecular-weight model compounds for the dienes incorporated in EPDM, selectively hydrogenated dienes were used. 5,6-Dihydrodicyclopentadiene (DCPDH) was used as a compound model for DCPD, 5-ethylidene-2-norbornane (ENBH) for ENB, and 5-vinylidene-2-norbornane (VNBH) for VNB (*Fig. 6.1*). These alkenes have different structures. Firstly, VNBH has one allylic H-atom, while DCPDH and ENBH have three and five allylic H-atoms respectively (bridgehead H-atoms are not included). Secondly, VNBH has a terminal unsaturation, while ENBH and DCPDH have an internal unsaturation. Linear or branched alkanes were used to mimic the characteristic moieties of the EPM backbone. The reaction products of the alkane/alkene/DCP mixtures were separated both by GC and by GC×GC and were identified by studying their MS-fragmentation patterns and their highly structured GC×GC chromatograms. The results of the model reactions will be presented systematically, starting with the identification of the products in the reaction mixtures, followed by their quantification. The data obtained will be used to propose an improved and expanded reaction mechanism for peroxide cross-linking of EPDM.

## 6.2. Experimental

5-Ethylidene-2-norbornane (ENBH) and 5-vinylidene-2-norbornane (VNBH) were produced in the laboratory via selective hydrogenation of ENB and VNB (see *Fig. 6.1*), using Pt on activated carbon as catalyst in solution. 5,6-Dihydrodicyclopentadiene (DCPDH) was purchased from Tokyo Kasei Kogyo (Japan). The purity of ENBH, ENBH and DCPDH was > 95% (*w/w*), as determined by GC separation and flame ionisation detection (FID). The reaction mixtures were prepared by dissolving 5% (*w/w*) dicumylperoxide (DCP, bis( $\alpha$ , $\alpha$ -dimethylbenzyl)peroxide, > 98%, Merck, Darmstadt, Germany) in *n*-octane (> 99%) or *n*-decane (> 99%), both purchased from Fluka (Buchs, Switzerland) and adding up to 20% (*w/w*) alkene (DCPDH, ENBH or VNBH). The starting compositions of the different experiments are given in Table 6.1. A magnetic stirrer was used to homogenise these solutions in a nitrogen atmosphere at room temperature for 2 h in a 3-mL pressure-resistant vial closed by a PTFE cap. The mixtures were subsequently stirred and heated for 30 min in an oil bath at

160°C. The reaction times were designed in order to accomplish total decomposition of the peroxide at the specified temperature (half-life time of the peroxide is 193 s at 160°C).

*Table 6.1. Starting compositions (% w/w) of the different reaction mixtures*

Experimental number	DCP	<i>n</i> -Octane	<i>n</i> -Decane	DCPDH	ENBH	VNBH
1	5.0	95.0				
2	5.0		95.0			
3	5.0	92.0			3.0	
4	5.0	88.0			7.0	
5–6	5.0	85.0			10.0	
7	5.0	75.0			20.0	
8	5.0		82.7		12.3	
9–10	5.0	86.0		9.0		
11	5.0	85.0		10.0		
12–14	5.0	86.0				9.0
15	5.0		84.1			10.9

The GC–MS experiments were performed on an Agilent 6890 GC and an Agilent 5973 MSD system (Agilent, Avondale, PA, USA). The capillary column used was a CP-Sil 5 CB low-bleed MS (100% dimethylpolysiloxane phase, 325°C maximum, 30.0 m × 0.25 mm,  $d_f$  0.25  $\mu$ m)(Varian, Palo Alto, CA, USA). The GC oven was programmed from 40°C (1 min isothermal) to 280°C at a rate of 1°C/min. The constant helium flow was 1 mL/min (49 kPa, vacuum outlet). The samples were injected undiluted using a split injection (split ratio 25:1) at 250°C. The quantification experiments were performed using the same GC system, equipped with an FID instead of the MS-detector. The FID-signal was collected with a data-management system (Atlas 2002, version 6.18, Thermo Labsystems, Manchester, UK).

The GC×GC–MS set-up consisted of an Agilent 6890N GC system and a Leco Pegasus III time-of-flight MS (St. Joseph, MI, USA). A non-polar capillary column VF-1MS (100% dimethylpolysiloxane phase, 50 m × 0.25 mm,  $d_f$  0.40  $\mu$ m; Varian) was used for the first separation dimension and a medium-polar capillary column VF-17MS (50% phenyl and 50% dimethylpolysiloxane phase, 1.5 m × 0.1 mm,  $d_f$  0.2  $\mu$ m; Varian) was used for the second dimension. The columns were coupled using a press-fit connection (Varian). The constant helium flow was 1.2 mL/min. The samples were injected undiluted using a split injection (split ratio 1:100) at 280°C. The GC oven was programmed from 40°C

(3 min isothermal) to 300°C (10 min isothermal) at 2°C/min. The second-dimension column temperature was maintained 5°C above that of the first-dimension column during the entire experiment. The modulator offset was 20°C. The MS was scanned from 20 to 550  $m/z$  at a rate of 150 spectra/s. The ion source was set at 250°C and the ionisation energy was 70 eV.

Size-exclusion chromatography (SEC) measurements were carried out to study the occurrence of higher molecular weight compounds (multiple-reaction products). The SEC separations were performed with four 7.8 mm x 300 mm Styragel columns placed in series (2\* HR0.5-HR1-HR2, Waters Corporation, Milford, Massachusetts, USA) at 50°C. THF was used as an eluent at a flow rate of 1 mL/min. Sample concentrations of approximately 0.5% ( $w/v$ ) and injection volumes of 40  $\mu\text{L}$  were used. The SEC-system consisted of a 515 HPLC Pump, 2410 Refractive Index detector, 2487 UV-detector ( $\lambda=254$  nm) and a 717 Plus Autosampler (Waters). The LC-system was controlled using Waters Empower software.

## 6.3. Results

### 6.3.1. Qualitative analysis of alkane/alkene/DCP reaction products

To study the combination and addition reactions, different mixtures of alkane/alkene/DCP were analysed by both GC–MS and GC $\times$ GC–MS before and after reaction. A typical GC–MS and GC $\times$ GC–MS chromatogram of a reaction mixture (*n*-octane and ENBH with DCP, Table 6.1, Experiment 5) is shown in Figs. 6.3 and 6.4, respectively. In all reaction mixtures the concentration of DCP after reaction was less than 0.1% ( $w/w$ ). Besides the starting alkane and alkene and the DCP decomposition products (2-phenylpropan-2-ol and acetophenone), three main clusters of reaction products can be distinguished in the GC and GC $\times$ GC chromatograms of the different mixtures. The identification of the various reaction products in the different clusters is illustrated using the reaction products of *n*-octane, ENBH and DCP (Table 6.1, Experiment 5) as an example. The reaction products with *n*-decane instead of *n*-octane and VNBH and DCPDH instead of ENBH have been identified in the same way.

The first cluster (**I**, Figs. 6.3 and 6.4) consists of the combination products of two octyl-radicals. The corresponding MS-spectra show a molecular ion peak at  $m/z$   $\text{C}_{16}\text{H}_{34}^{\bullet+} = 226$ . A mixture of octane dimers is found, as hydrogen abstraction can take place from each C-atom in *n*-octane and each resulting

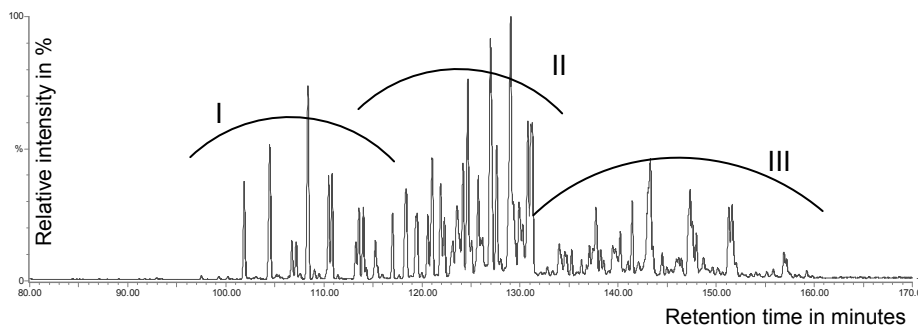


Fig. 6.3. GC-MS chromatogram with three different clusters of reaction products of *n*-octane with 10% (w/w) ENBH and 5% (w/w) DCP (Table 6.1, Experiment 5). See experimental section for GC-MS conditions.

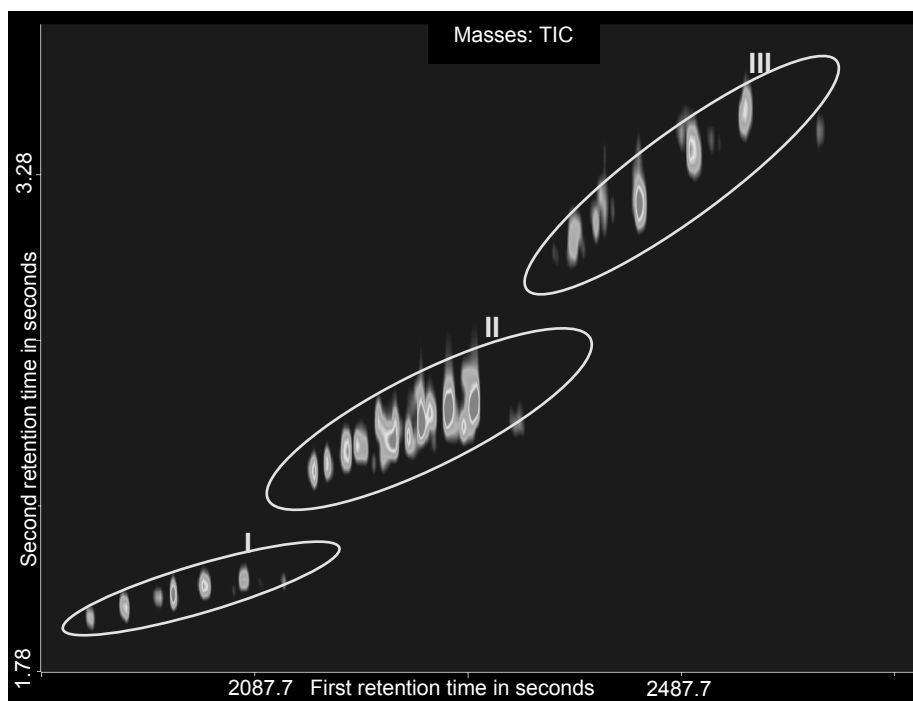


Fig. 6.4. GCxGC-TOF-MS chromatogram with three different clusters of reaction products of *n*-octane with 10% (w/w) ENBH and 5% (w/w) DCP (Table 6.1, Experiment 5). See experimental section for GCxGC-TOF-MS conditions.

octyl-radical can participate in a combination reaction. The different branching positions of these dimers have been elucidated as described in our previous study [12]. The structure of the dimers and the MS-characteristics ( $m/z$  ions) of

cluster **I** are given in Table 6.2. In comparison with a statistical distribution, a higher reactivity for hydrogen abstraction from the methylene group next to a primary methyl group ( $\text{CH}_3\text{-CH}_2\text{-CH}_2\text{-R}$ ) and a lower reactivity from the methylene group next to an ethyl group ( $\text{CH}_3\text{-CH}_2\text{-CH}_2\text{-CH}_2\text{-R}$ ) are observed. This is in line with previous research [12] and is probably due to steric hindrance and entropy effects.

Table 6.2. EI-MS-identified reaction products (cluster **I**) of *n*-octane with 10% (w/w) ENBH and 5% (w/w) DCP

Peak Number	$M_w$ (Da)	Characteristic octane dimer $m/z$ ions	Structure octane dimers ( <sup>a</sup> )	Branching positions in <i>n</i> -octane
1	226	127, 169, 183	10_05(C3)06(C3)	C4-C4
2	226	127, 155, 169, 183, 197	11_05(C3)06(C2)	C4-C3
3	226	127, 155, 197	12_06(C2)07(C2)	C3-C3
4	226	127, 141, 169, 183	12_05(C3)06(C1)	C4-C2
5	226	127, 141, 155, 197	13_06(C2)07(C1)	C3-C2
6	226	127, 169, 183	13_05(C3)	C4-C1
7	226	141	14_07(C1)08(C1)	C2-C2
8	226	127, 155, 197	14_06(C2)	C3-C1
9	226	141	15_07(C1)	C2-C1
10	226	127, 141, 155, 169, 183, 197	16	C1-C1

<sup>a</sup> The first two digits (xx\_xx(Cx)xx(Cx)) indicate the length of the hydrocarbon backbone; each next two digits (xx\_xx(Cx)xx(Cx)) show the position of the side chain on the backbone, while the length of the side chain is given between brackets (xx\_xx(Cx)xx(Cx)).

The second cluster (**II**, Figs. 6.3 and 6.4) corresponds mainly to products with a molecular ion peak at  $m/z$   $\text{C}_{17}\text{H}_{30}^{\bullet+} = 234$ . These chromatographic peaks are representative of products formed by the combination of *n*-octane-radicals and ENBH-radicals (Fig. 6.5, peaks designated 11–24). The different isomers are explained by the different reaction positions of *n*-octane, but also due to the different reaction positions of ENBH. To obtain more insight in the chemistry and the reactivity of the radicals formed upon hydrogen abstraction from ENBH and *n*-octane, the electron-ionisation (EI)–MS fragmentation of these isomeric structures was studied in more detail. The position where the *n*-octane had reacted could be established using the high-mass ions ( $m/z = 219, 205, 191, 177, 163, 149$  and  $135$ ). In general, the EI-MS spectra of these reaction products are dominated by abundance maxima at  $m/z$   $\text{C}_3\text{H}_7^+ = 43$ ,  $m/z$   $\text{C}_4\text{H}_9^+ = 57$ , and  $m/z$

$C_3H_{11}^+ = 71$  ions, and they show some characteristic ions at  $m/z$  71,  $m/z$  93/94 and  $m/z$  121/122.

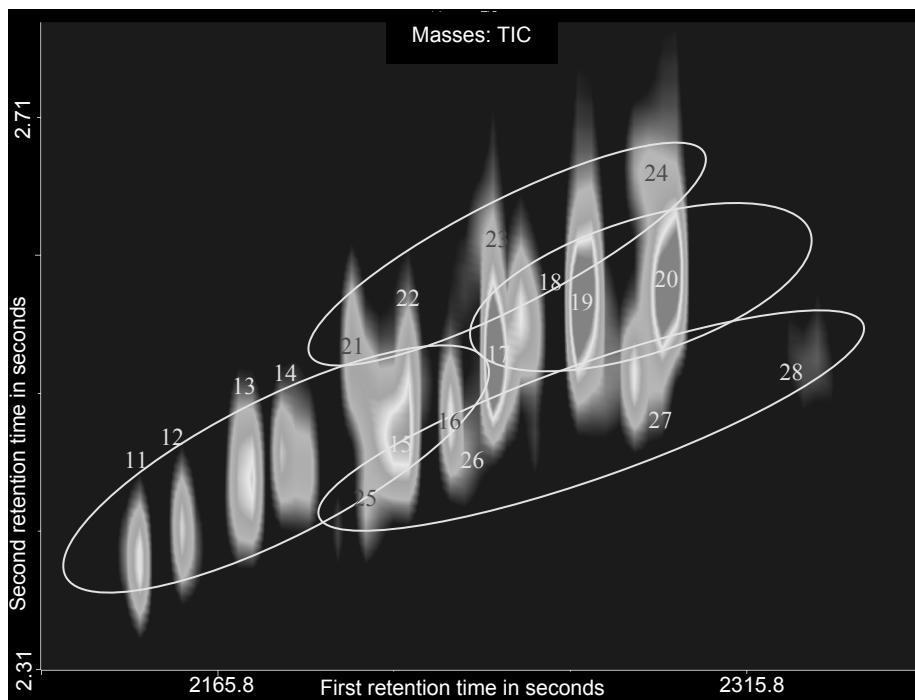


Fig. 6.5. Enlargement of GCxGC-TOF-MS chromatogram of cluster II of reaction products of *n*-octane with 10% (w/w) ENBH and 5% (w/w) DCP (Table 6.1, Experiment 5).

The MS-spectra of the group with chromatographic peaks 11–16 contain highly abundant ions at  $m/z$  94 and 122, as shown in the typical MS-spectrum in Fig. 6.6a. The MS-spectra of the second group with chromatographic peaks 17–20 show highly abundant ions at  $m/z$  = 93 and 121, as shown in the typical MS-spectrum in Fig. 6.6b. These ions indicate the branching position of ENBH, as proposed in the MS-fragmentation mechanism in Fig. 6.7. The chromatographic peaks with  $m/z$  94 and 122 are indicative of hydrogen abstraction from the allylic position located in the ring (branching position C3 of ENBH), while the chromatographic peaks with  $m/z$  93 and 121 are indicative of hydrogen abstraction from the exocyclic allylic position (branching position C9 of ENBH). The MS-spectra of peaks 21–24 show a highly abundant  $m/z$  94 ion, which indicates combination products ( $M_w = 234$  Da) from ENBH-radicals, resulting from hydrogen abstraction from alkylic carbons of ENBH.

Table 6.3. EI-MS-identified reaction products (cluster II) of *n*-octane with 10% (w/w) ENBH and 5% (w/w) DCP

Peak Number	$M_w$ (Da)	Characteristic ENBH $m/z$ ions	Branching position of ENBH	Characteristic <i>n</i> -octane $m/z$ ions	Branching position of <i>n</i> -octane
11	234	94/122	C3	177/191	C4
12	234	94/122	C3	177/191	C4
13	234	94/122	C3	163/205	C3
14	234	94/122	C3	163/205	C3
15	234	94/122	C3	149	C2
16	234	94/122	C3	149	C2
17	234	93/121	C9	177/191	C4
18	234	93/121	C9	177/191	C4
19	234	93/121	C9	163/205	C3
20	234	93/121	C9	149	C2
21	234	94	C5 or C6 or C7	177/191	C4
22	234	94	C5 or C6 or C7	163/205	C3
23	234	94	C5 or C6 or C7	149	C2
24	234	94	C5 or C6 or C7	--	C1
25	236	123	C2 or C8	179/193	C4
26	236	123	C2 or C8	165/207	C3
27	236	123	C2 or C8	151	C2
28	236	123	C2 or C8	--	C1

The bridgehead CH-atoms of ENBH (positions C1 and C4) are not susceptible to hydrogen abstraction, because the resulting alkyl-radicals cannot attain a planar configuration [16]. Therefore, only alkyl-radicals will be formed by hydrogen abstraction from positions C5, C6, and/or C7. Peaks 25–28 (Fig. 6.5) show molecular ions at  $m/z$  236 ( $C_{17}H_{32}^{\bullet+}$ ). These reaction products are formed by the addition reaction of *n*-octyl-radicals to ENBH at the olefinic positions C2 and C8. The molecular weights, the characteristic ions, and the branching positions of the corresponding peaks in the different groups are given in Table 6.3. The identified octane–ENBH reaction products show GC×GC elution patterns, that agree very well with the expected elution order. Since the GC×GC analysis is based on subsequent separations according to boiling point (first-dimension) and polarity (second-dimension), the retention in both dimensions increases with decreasing length or number of the side chains. The addition products elute later in the first-dimension, since their molecular weight is higher than that of the products of combination reactions. In contrast, retention in the second-dimension decreases, due to the absence of the unsaturation.

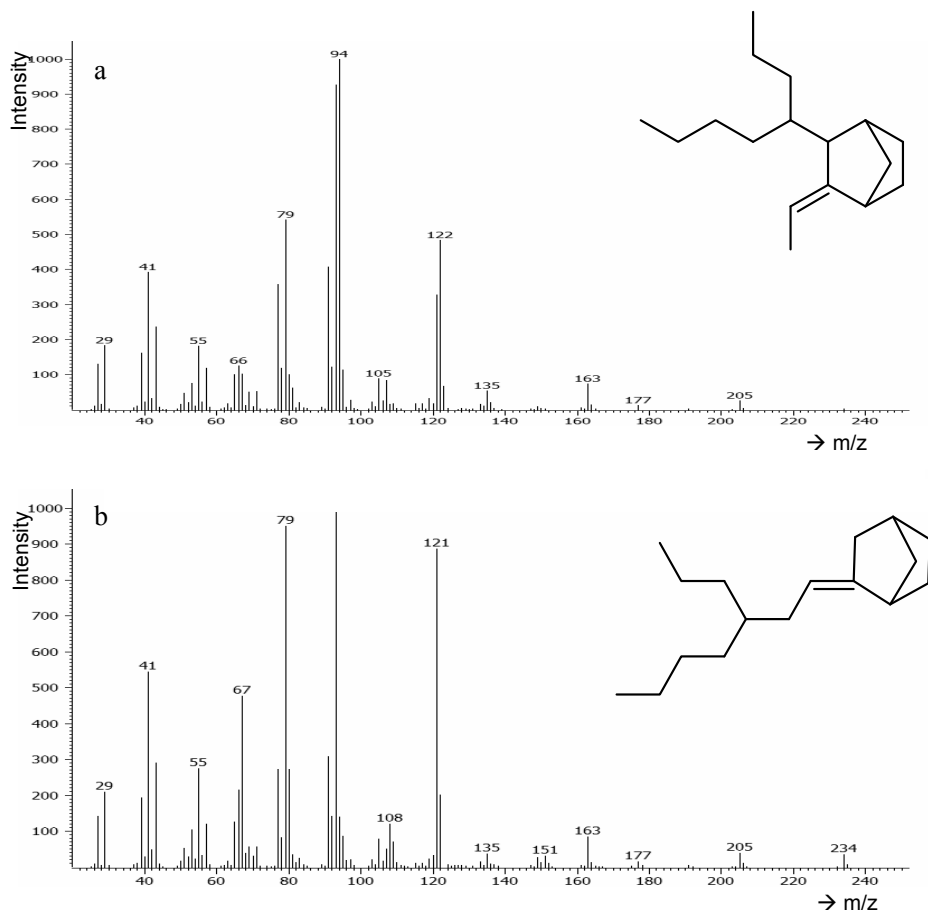


Fig. 6.6. Typical EI-MS-spectra of combination products of ENBH and *n*-octane. MS-spectrum 6.6a (peak 12 of cluster **II**) indicating hydrogen abstraction from ENBH at position C3, while MS-spectrum 6.6b (peak 19 of cluster **II**) indicating hydrogen abstraction from ENBH at position C9.

The structures of the identified reaction products show that hydrogen abstraction from the allylic positions in the ENBH ring (position C3) and from the allylic group (position C9) is strongly preferred to hydrogen abstraction from the alkylic C- atoms at positions C5, C6 and C7 in the ENBH ring. The allylic positions C3 and C9 are more susceptible to hydrogen abstraction than the other C-atoms, because the formed allylic-radical is stabilised via conjugation with the double bond. This was confirmed by calculated<sup>1</sup> and published bond-dissociation energies [16,17] for the different ENBH positions. Finally, no indication was found for hydrogen abstraction from the primary CH<sub>3</sub> groups of

*n*-octane, in contrast with the experiments with DCP and *n*-octane only, in which low concentrations of products arising from primary octyl-radicals were found.

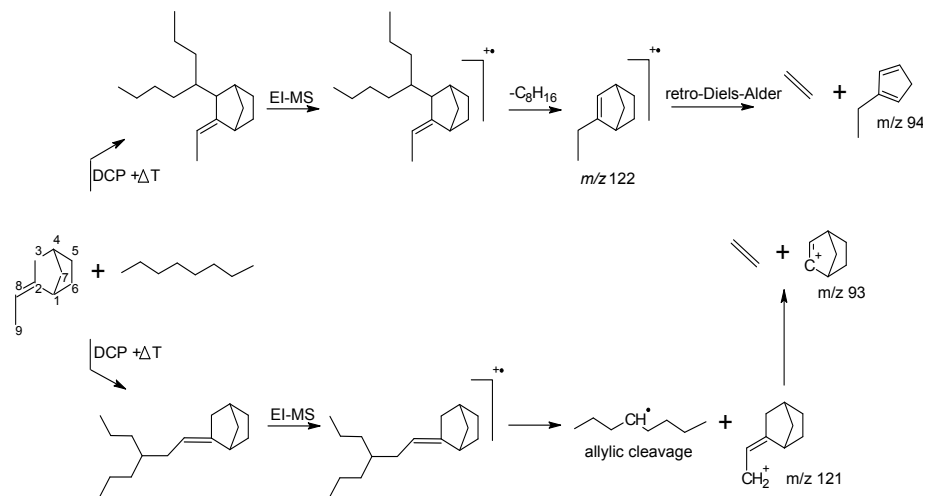


Fig. 6.7. MS-fragmentation mechanism of *n*-octane/ENBH combination products, showing the C3 and C9 branching positions of ENBH.

The third cluster (**III**, Figs. 6.3 and 6.4) is dominated by peaks with a molecular ion of  $m/z$  C<sub>18</sub>H<sub>24</sub><sup>•+</sup> = 242. This corresponds to combination products of two ENBH-radicals (Fig. 6.8, peaks designated 29–31). At lower concentrations the addition products of an ENBH-radical and an ENBH molecule are observed ( $m/z$  C<sub>18</sub>H<sub>26</sub><sup>•+</sup> = 244, Fig. 6.8, peaks designated 32–35). The three main peaks, corresponding to combination products, show a neutral loss of 28 Da from the molecular ion and abundance ion peaks at  $m/z$  = 67, 93, and 121. Based on the EI-MS fragmentation, these peaks are identified as outlined in Table 6.4.

The MS-spectra of the addition products are dominated by highly abundant ions with  $m/z$  C<sub>5</sub>H<sub>7</sub><sup>+</sup> = 79 and the neutral loss of 28 Da (C<sub>2</sub>H<sub>4</sub>). This strong neutral loss from the molecular ion appears to arise from initial migration of the double bond away from the position of branching during EI-MS fragmentation. This renders these MS-spectra less reliable for the identification of the branching structure in ENBH/ENBH addition products.

<sup>1</sup> The bond dissociation energy calculations were performed using Chremdraw Ultra 10 (CambridgeSoft Corporations) with B3LYP functional and a 6-31G(\*) basis set. The calculations have been performed in *n*-octane as solvent.

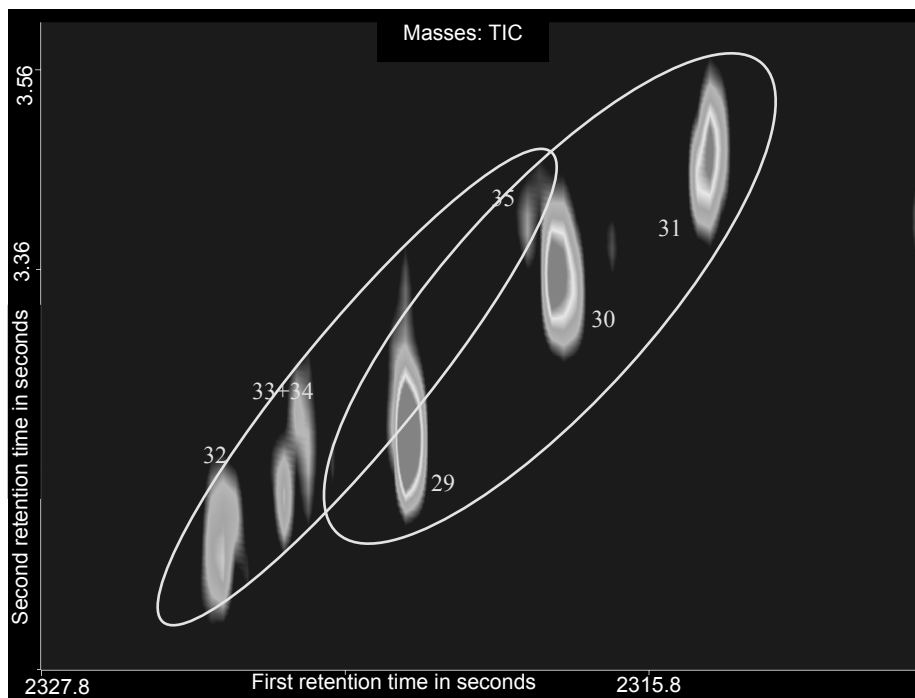


Fig. 6.8. Enlargement of GC×GC–TOF–MS chromatogram of cluster **III** of reaction products of *n*-octane with 10% (w/w) ENBH and 5% (w/w) DCP (Table 6.1, Experiment 5).

The GC–MS and the GC×GC–MS chromatograms give no indication of higher molecular weight compounds (multiple-reaction products). However, it is questionable if higher molecular weight compounds can be analysed by GC. Therefore SEC analyses have been performed. SEC analyses gave no indication of trimers and higher oligomers. Although the presence of these compounds at low concentrations cannot be totally excluded, their concentration is less than 1% (w/w) of the formed products. No reaction products of a methyl-radical and/or a cumyloxy-radical with an alkene were observed. Thus, no addition of peroxide-derived radicals to the alkene unsaturation took place. Finally, unsaturated reaction products ( $C_{16}H_{32}$  or  $C_8H_{16}$ ) and/or low-molecular-weight products ( $< C_8$ ) derived from octane were not observed, which indicates that disproportionation and/or scission reactions do not occur significantly (less than 1% (w/w) of the formed products).

The reaction mixtures of DCP, *n*-octane or *n*-decane, and DCPDH or VNBH gave similar reaction products as found for ENBH. A large variety of combination products of two alkyl-radicals, two allyl-radicals, or an allyl-radical and an alkyl-radical were observed, as well as addition products of alkyl- and

allyl-radicals with the alkene.

Table 6.4. EI-MS-identified reaction products (cluster III) of *n*-octane with 10% (w/w) ENBH and 5% (w/w) DCP

Peak Number	$M_w$ (Da)	Characteristic ENBH $m/z$ ions	Branching position of ENBH
29	242	93/121	3/3
30	242	93/121	9/3
31	242	93/121	9/9
32-35	244	79/93/121/214	?

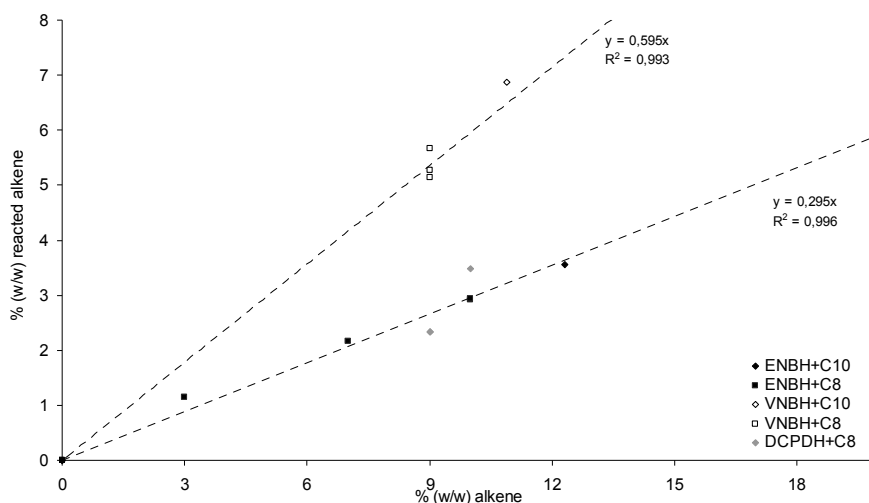


Fig. 6.9. Percentage of reacted alkene vs. the starting concentration (% w/w) of alkene for different model experiments.

### 6.3.2. Quantitative analysis of alkane/alkene/DCP reaction products

The different “cross-linked” reaction products of the mixtures of alkanes, alkenes, and DCP were quantified using GC-FID. The concentrations of reacted alkane and alkene were quantified in two different ways. The decrease in the concentration after reaction (conversion) was determined, as well as the concentrations of formed products. The two quantification procedures resulted in similar concentrations of the reacted alkanes and alkenes. The “cross-linking” experiments performed in triplicate (Table 6.1, Experiments 12–14) indicate a



respectively. There are no significant differences in the total concentrations of combination products between ENBH, DCPDH, and VNBH (see *Fig. 6.11*). The total concentration of combination products is also not affected by the alkane used ( $n\text{-C}_8$  vs.  $n\text{-C}_{10}$ ), and it is actually similar to the concentration of combination of alkanes in the absence of an alkene (*Fig. 6.11*; Table 6.1, Experiments 1 and 2). The similar concentrations of combination products in the experiments with different alkenes suggest that the number of allyl H-atoms in the alkene is not relevant. The determining factor for the total concentration of combination products is the number of useful free radicals, which are formed by hydrogen abstraction either directly by the peroxide-radicals or by radicals formed during the addition reaction. Apparently, the number of effective radicals is simply determined by the concentration of peroxide-radicals, which was constant in this study.

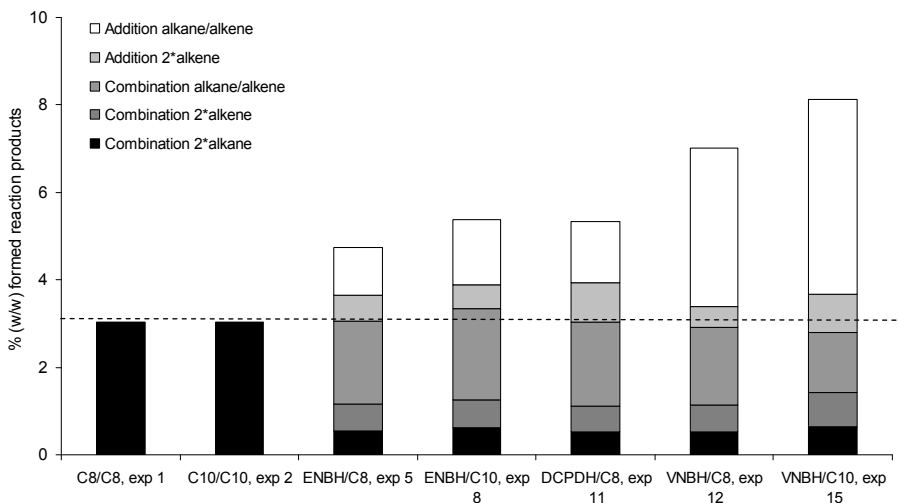


*Fig. 6.11. Concentration of reaction products of ENBH, DCPDH and VNBH in alkane with DCP.*

*Fig. 6.11* also shows that VNBH has a higher susceptibility to the addition by an alkyl-radical than ENBH and DCPDH, resulting higher concentrations of reacted VNBH in comparison with ENBH or DCPDH, at the same starting concentration of alkene (*Fig. 6.9*). The concentration of reacted alkane is slightly lower for VNBH compared to ENBH and DCPDH (*Fig. 6.10*). This demonstrates the high reactivity of the VNBH terminal unsaturation for radical addition in comparison with the more sterically hindered internal unsaturations of ENBH and DCPDH alkenes, despite the low number of allylic H-atoms of VNBH compared to ENBH.

In addition to experiments with different types of alkenes, experiments were performed with different concentrations of ENBH in *n*-octane (Table 6.1, Experiments 1 and 3-7). The amounts of *n*-octane and ENBH involved in the addition and combination reactions were calculated using the quantitative data described above. They are plotted versus the starting concentration of ENBH in *Fig. 6.12*. The total concentrations of combination products, using VNBH or DCPDH as alkene, are also shown in *Fig. 6.12*, although only one experiment at one concentration level was performed. The data show that the total concentration of combination products is independent of the concentration of ENBH used. From the single experiments using VNBH and DCPDH, it seems that the concentration of combination products is also independent of the type of alkene used (VNBH, ENBH or DCPDH). The total concentration of addition-reaction products increases with the initial concentration of alkene.

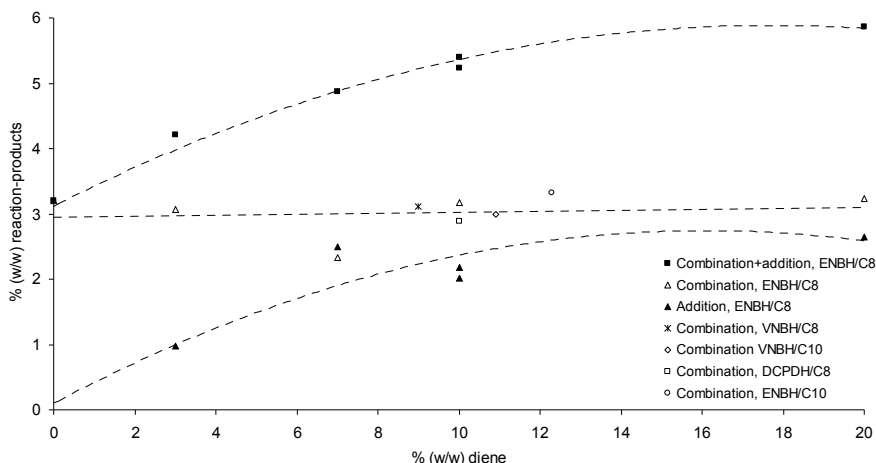


*Fig. 6.12. Concentration of combination and addition products vs. starting concentration of alkene for different model experiments.*

From the experiments with different types and concentrations of alkenes, it can be concluded that the total concentration of combination products depends only on the DCP (peroxide) content and on the peroxide cross-linking efficiency. The latter is defined as the number of moles of cross-linked products formed per mol of peroxide. The peroxide efficiency for DCP in the absence of an alkene is approximately 72%. The peroxide efficiency increases with increasing concentration of alkene up to 114% for 9% (w/w) ENBH. The peroxide efficiency for VNBH is even higher, *i.e.* 173% for 9% (w/w) VNBH. This

indicates that the addition reaction has a cyclic character and that it yields a contribution to the total cross-link density that is greater than just the combination reaction. After the addition of a radical to an alkene, the intermediate radical abstracts hydrogen from another alkane or alkene. This new radical can combine with another radical (combination) or react with another alkene (addition). The average number of repetitions of the addition reaction is about 0.6 for 9% (w/w) ENBH and about 1.4 for 9% (w/w) VNBH. From this it can be calculated that the susceptibility of VNBH to hydrogen abstraction is about 14 times greater than that of an alkane, while the susceptibility of ENBH is about 5 times greater than that of an alkane. From this it can be calculated that the probability of hydrogen abstraction from allylic positions in alkenes is about 26 times and about 129 times greater for ENBH and VNBH, respectively, than from aliphatic positions in alkanes and alkenes.

### **6.3.3. Cross-linking mechanism of EPDM**

The generally accepted mechanism for peroxide cross-linking of EPDM consists of cross-linking through combination of two EPDM macro-radicals and through the addition of an EPDM-radical to an EPDM unsaturation (*Fig. 6.2*). This study with low-molecular-weight model compounds reveals that both alkyl- and allyl-radicals are formed, from the alkane and from the residual unsaturation respectively. This actually results in five different cross-linking reactions, *viz.* the addition of an allyl- or an alkyl-radical to the unsaturation of the alkene and the combination of two alkyl-radicals, two allyl-radicals, or an allyl-radical and an alkyl-radical. Thus, the combination reaction also involves the unsaturated compound, despite its low concentration. This is because the susceptibility to hydrogen abstraction is much greater for allylic carbons than for alkylic ones. The combination reaction is independent of the concentration and the type of diene used and it is probably simply determined by the concentration of peroxide. These observations are totally in line with the experimental observations of van Duin and Dikland [4], who found fixed cross-link densities resulted from combination reactions using different types (DCPD, VNB, ENB) and concentrations of dienes. The use of an alkene with a less sterically hindered unsaturation (*e.g.* VNBH) results in a higher frequency of addition reactions, while the ease of hydrogen abstraction of allylic H-atoms is not the determining factor for the cross-linking efficiency. This is due to the fact that the addition reaction is cyclic. After the addition reaction, hydrogen transfer takes place and the radical formed can combine with another radical (combination) or add to a diene (addition). These results agree well with the total cross-linking densities of

EPDM/peroxide rubbers with VNB, ENB or DCPD as dienes, as determined by rheometry [3].

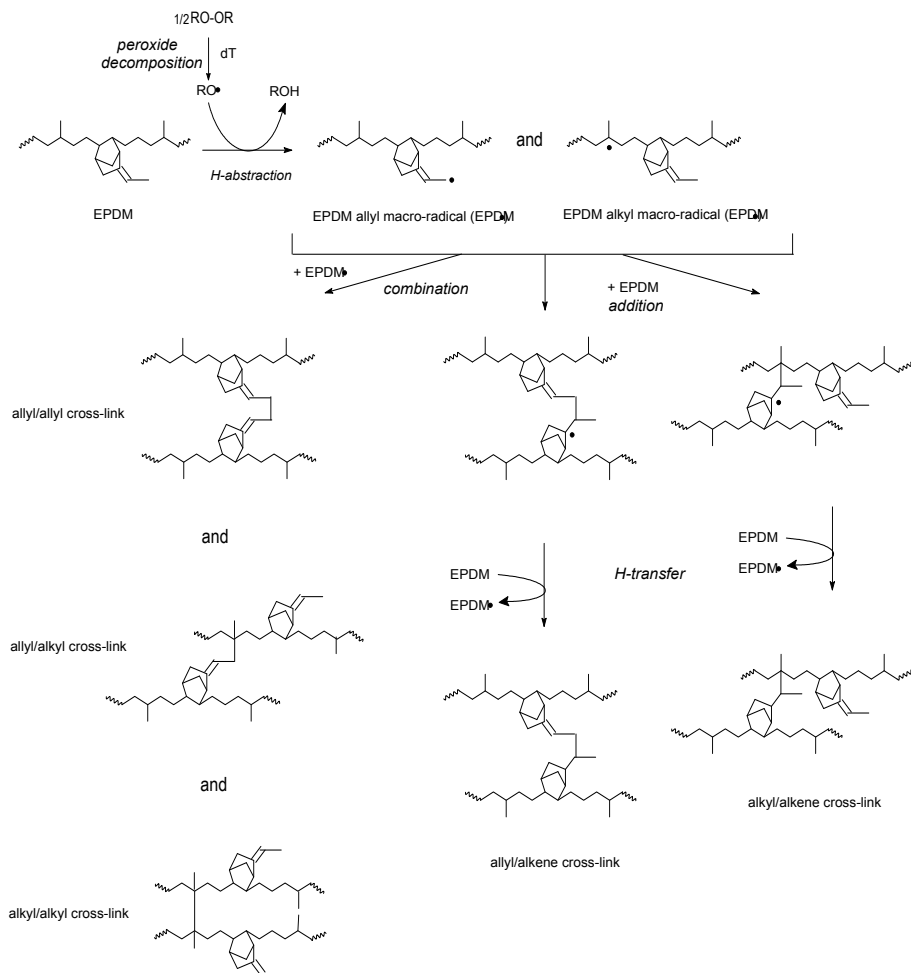


Fig. 6.13. Extended reaction scheme for peroxide cross-linking of EPDM with ENB as a diene.

Although the results of the present model study with low-molecular-weight compounds should be translated to the EPDM rubber system with some care, the observations are totally in line with other experimental observations on peroxide cross-linking of EPDM [3-6]. Based on the new results the peroxide cross-linking reaction mechanism for EPDM should be extended (Fig. 6.13).

## 6.4. Conclusion

The peroxide cross-linking reaction of EPDM has been studied using different concentrations of low-molecular-weight alkenes dissolved in alkanes, representing the characteristic structural units in EPDM rubber. These mixtures were “cross-linked” with DCP under conditions as close as possible to those encountered during actual cross-linking of EPDM. Analysis of the formed reaction products by GC–MS and GC×GC–MS revealed five classes of reaction products, *viz.* three types of combination products (two alkyl-radicals, two allyl-radicals, or one allyl-radical with an alkyl-radical) and two types of addition products (alkyl- or allyl-radicals with the alkene). Although GC×GC is not necessary to improve the GC-separation, the highly structured GC×GC chromatogram confirms the different isomeric reaction products derived from MS-fragmentation patterns. Based on these identified compounds, the peroxide cross-linking reaction mechanism for EPDM is expanded to that outlined in *Fig. 6.13*.

Quantification of the different reaction products showed the combination reaction to be independent of the concentration and structure of the alkene (ENBH, VNBH and DCPDH). The concentration of the addition products is influenced by the concentration and by the structure of the alkene. An increase in the alkene concentration results in an increase in the concentration of addition products. VNBH is more prone to addition reactions than ENBH or DCPDH, which is in agreement with peroxide cross-linking efficiency studies of EPDM and which can be explained by less steric hindrance of the terminal VNBH unsaturation.

This study with low-molecular-weight model compounds has resulted in a more accurate structural characterisation of the products of peroxide curing, and in a more detailed description of the mechanism of peroxide cross-linking of EPDM. It is concluded that the use of low-molecular-weight compounds to mimic the cross-linking of EPDM, followed by GC–MS and GC×GC–MS analysis, forms a very powerful tool to study rubber cross-linking mechanisms and the resulting cross-linked structures.

## References

- [1] J.A. Brydson, *Rubbery Materials and their Compounds*, Elsevier, London, 1988.

- [2] W. Hofmann, *Kautsch. Gummi Kunstst.* 40 (1987) 308.
- [3] M. van Duin, M. Dees, H. Dikland, Fall 172<sup>nd</sup> Technical Meeting of the Rubber Division of the American Chemical Society, Inc. Cleveland, OH, October 16-18, 2007, ISSN:1547-1977.
- [4] M. van Duin, H.G. Dikland, *Rubber Chem. Technol.* 76 (2003) 132.
- [5] F.B. Baldwin, P. Borzel, C.A. Cohen, H.S. Makowski, J.F. van Castle, *Rubber Chem. Technol.* 43 (1970) 522.
- [6] V.M. Litvinov, W. Barendswaard, M. van Duin, *Rubber Chem. Technol.* 71 (1998) 105.
- [7] V.M. Litvinov, M. van Duin, *Kautsch. Gummi Kunstst.* 55 (2002) 460-462.
- [8] V. Livinov, *Macromolecules* 39 (2006) 8727-8741.
- [9] H.G. Dikland, *Coagents in peroxide vulcanisations of EP(D)M rubber*, Thesis, 1992. University of Twente, Enschede, The Netherlands, ISBN:90-9005615-7.
- [10] H.M. van den Berg, J. W. Beulen, E.F.J. Duynstee, H.L. Nelissen, *Rubber Chem. Technol.* 57 (1984) 265.
- [11] S. Camara, B.C. Gilbert, R.J. Meier, M. van Duin, A.C. Whitthood, *Org. Biomol. Chem.* 1 (2003) 1181-1190.
- [12] R. Peters, D. Tonoli, M. van Duin, J. Mommers, Y. Mengerink, A.T.M. Wilbers, R. van Benthem, C.G. De Koster, P. J. Schoenmakers, S. van der Wal, *J. of Chromatogr. A*, 1201 (2008)141-150.
- [13] J.B. Phillips, J. Beens, *J. Chromatogr. A* 856 (1999) 331.
- [14] M. van Deursen, J. Beens, J. Reijenga, P. Lipman, C. Cramers, J. Blomberg, *J. of High Resol Chrom.* 23 (2000), 507-510.
- [15] R. Edam, J. Blomberg, H.-G. Janssen, P.J. Schoenmakers, *J. Chromatogr. A* 1086 (2005) 12-20.
- [16] J.K. Kochi (Ed), *Free radicals*, vol. 1, John Wiley & Sons, New York, 1973.
- [17] D.G. Hendry, T. Mill. L. Piszkiwicz, J.A. Howard and H.K. Eigenmann, *J. Phys. Chem. Ref. Data.* 3 (1974) 937.